

# In-situ synthesis of gold nanoparticles using an aerosol-assisted atmospheric pressure cold plasma

A. Bjelajac<sup>1</sup>, A.-M. Phillipe<sup>1</sup>, J. Guillot<sup>1</sup>, J.-B. Chemin<sup>1</sup>, P. Choquet<sup>1</sup> and S. Bulou<sup>1</sup>

<sup>1</sup> Luxembourg Institute of Science and Technology, MRT, 28, avenue des Hauts-Fourneaux, L-4365 Esch-sur-Alzette, Luxembourg

**Abstract:** Herein, we demonstrate the benefit of applying plasma during in-situ synthesis of gold nanoparticles using an atmospheric pressure DBD plasma torch and an aerosol of  $\text{HAuCl}_4 \cdot 3\text{H}_2\text{O}$  solution as gold precursor. Using a pure ethanol-based solution with plasma applied, a carbon-based matrix around the gold nanoparticles was created which prevented the gold NPs from agglomerating. XPS analyses confirmed that plasma induced the complete reduction of Au. These findings are supported by detailed HRTEM and SAED results.

**Keywords:** atmospheric pressure plasma, PECVD, aerosol, gold nanoparticles, TEM, XPS.

## 1. Introduction

Due to wide range of application of gold (Au) nanoparticles (NPs), ranging from medical therapy [1] and drug delivery [2] to chemical sensing [3] and catalysis [4], efforts are made in finding a controllable one-step method that can ensure the narrow size distribution and well dispersion of Au NPs. It is also important to provide the NPs surface modification, i.e. labelling by an organic drug molecule. These criteria are met by using a stabilizer agent, commonly a bio-ligand, such as polyvinylpyrrolidone (PVP) [5] or poly(ethylene glycol) (PEG) [6]. However, the optimization of the capping agent concentration is required since it affects the NPs stability, size, and distribution. Therefore, the advantage is given to finding a ligand-free method of Au NPs synthesis and one of them is the atmospheric pressure cold plasma process proposed by Mariotti et al [7]. In the following work of this research team, Maguire et al demonstrated the synthesis of 5 nm Au NPs created “in-flight” from microdroplets of  $\text{HAuCl}_4$  aqueous solution [8]. The He/Ne gas stream transported the droplets along the tube to the plasma region formed by concentric ring electrodes at the outer wall and driven by rf power. Herein, we modified their approach by using an atmospheric pressure Dielectric Barrier Discharge (DBD) plasma torch where the Au NPs were produced due to the plasma discharge interactions with a nebulized Au precursor solution.

## 2. Experimental

The schema of the experimental set-up used here is given in Fig.1. The plasma is created between the inner quartz tube (6 mm outer diameter, 4 mm inner diameter, coated with Pt) and the outer plasma tube (9 mm outer diameter, 7 mm inner diameter, covered by Al foil which is connected to the HV generator). To produce the plasma, 10 slm of Ar is sent in the gap between the 2 tubes, and a sinusoidal HV is applied to the outer electrode (AFS generator, 52 kHz, 20 W). The inner hollow grounded tube is used to carry the nebulized Au precursor (0.25 g/L of  $\text{HAuCl}_4 \cdot 3\text{H}_2\text{O}$ ) solution in the near post-discharge. 10 slm of Ar was used as a carrier gas of Au precursor.

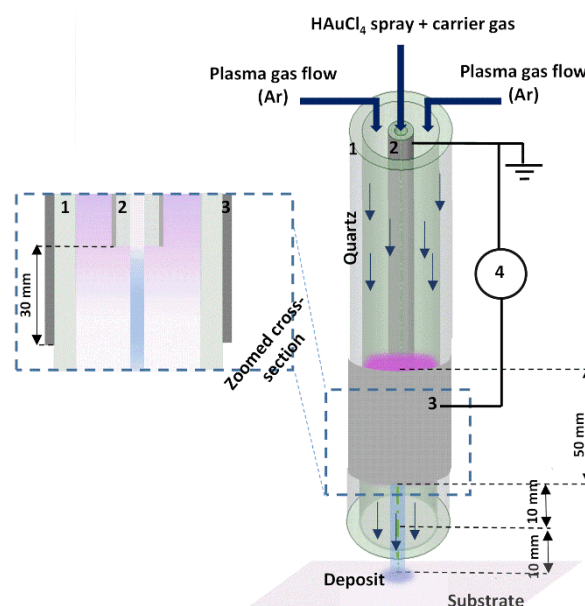


Fig. 1. Schema of the experimental set-up: 1: outer quartz tube, 2: inner injection tube with Pt coating, 3: Al foil and 4: generator.

The SEM investigations were carried out on a Hitachi SU-70 FE-SEM, whereas TEM analyses were done on a JEOL JEM-F200 cold FEG microscope operating at an acceleration voltage of 200 kV. Crystalline nanostructures were analyzed by direct spacing measurements on High-Resolution TEM (HRTEM) images as well as by Selected Area Electron Diffraction (SAED) using Digital Micrograph Software from Gatan (version v.3.50.3584.0). Energy dispersive spectroscopy (EDS) mapping was done in STEM mode.

X-ray photoelectron spectra were acquired using a Kratos Axis Ultra-DLD photoelectron spectrometer with a monochromatic Al K $\alpha$  source (10 mA, 15 kV) and a 700  $\mu\text{m} \times 300 \mu\text{m}$  spot size. Survey spectra were acquired using a pass energy of 160 eV, whereas high resolution spectra of the Au 4f, Cl 2p, C 1s, O 1s, and Si 2p regions were collected with a pass energy of 20 eV. The binding energies were referenced to the adventitious carbon at 285.0 eV. The shape of a reference spectrum acquired on a sputter-clean gold foil was used to fit the metallic Au 4f component. All other components were reconstructed using Gaussian-Lorentzian peaks after removing a Shirley type background.

### 3. Results and Discussion

Prior optimization of the precursor concentration and the deposition time was done to ensure the narrow size distribution of the obtained Au NPs. Also, we investigated the influence of solvent composition (water-ethanol ratio) and we chose to use pure ethanol based solution, since it provides the best dispersion of Au NPs as compared to water based solution. The role of ethanol was discovered to be essential since ethanol served as C source for creation of C matrix around Au NPs preventing them from agglomeration. Fig. 2 given an overview of results of Au NPs deposit obtained using 0.25 g/L precursor in pure ethanol, 10 mins of plasma deposition.

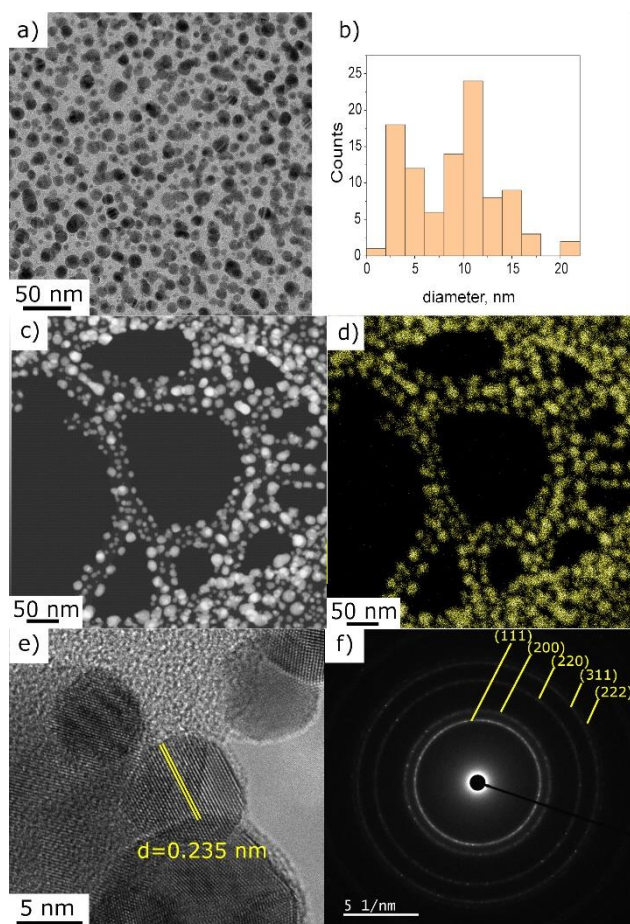


Fig. 2. a) TEM micrograph, b) NPs size distribution histogram, c) STEM micrograph and d) corresponding EDS mapping, Au signal, e) HRTEM with measured interplanar distance, f) SAED of the area given in a).

Without plasma applied during deposition (the same parameters), the obtained NPs were ~50 nm coming from the droplets drying, either in droplets' centre or at the border (marked with arrows on Fig. 3 a)). The TEM micrographs revealed two kinds of morphologies: the agglomerates (like the one circled in Fig.3 b) and the individual NPs (such as the presented one given in Fig 3.

d)). SAED analysis of one of these agglomerates is presented in Fig. 3 c). By exploring the different JCPD-ICDD cards (obtained experimentally or calculated), a close match was found with gold oxide chloride (JCPD-ICDD 04-012-8341 card<sup>23</sup>). In addition, the HRTEM image of one NP (Fig 3. d) shows, for instance, the 0.249 nm interatomic distance corresponding to the (23-1) plane of gold oxide chloride.

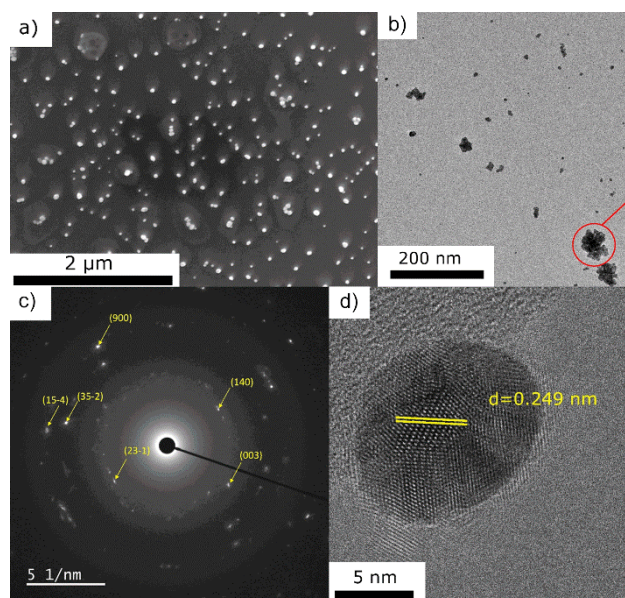


Fig. 3. SEM and TEM micrographs of Au deposit obtained using 0.25 g/l precursor in pure ethanol without applying plasma, 10 mins.

Further, XPS analyses were carried out to determine the chemical states of Au and Cl to get more insight into the molecular structure of the obtained deposits (without and with plasma applied, Fig. 4 a) and b), respectively). High resolution XPS spectrum of the Au 4f 7/2 of the no-plasma sample shows 2 components corresponding to Au (I), at 84.9 eV, and Au (III) at 87.4 eV [9]. Recalling the results of TEM and SAED analyses, we can assume that Au(III) component originates from AuOCl, whereas the Au(I) signal may be from AuCl. This was expected since it is well known that the precursor,  $\text{HAuCl}_4 \cdot 3\text{H}_2\text{O}$ , is metastable and is prone to be reduced [10]. However, in the case of plasma-treated sample, 3 contributions are identified as follows: the component at 84.0 eV matches well to bulk metallic Au and corresponds in this sample to Au(0) clusters electrically connected to the substrate [9]. The contribution at 84.4 eV, so with a +0.4 eV upward shift, can be due to metallic Au(0) particles embedded in a carbon matrix. Similar was reported for Au NPs with C-based capping agents [11]–[13]. To verify this hypothesis, we performed the XPS also on a deposit obtained using the same conditions but with the Au precursor dissolved in water. Indeed, the results showed that Au 4f position corresponds to Au(0) contribution only, without any shift,

as expected since without ethanol as a solvent, there was no C source for the creation of matrix around Au NPs.

The third and the smallest contribution at 86.2 eV can be associated to the coexistence of several phases as Au(III) (i.e. AuOCl, Au(OH)<sub>3</sub> or AuCl<sub>3</sub>) which are in contact with metallic Au, as already reported in literature [14]–[16].

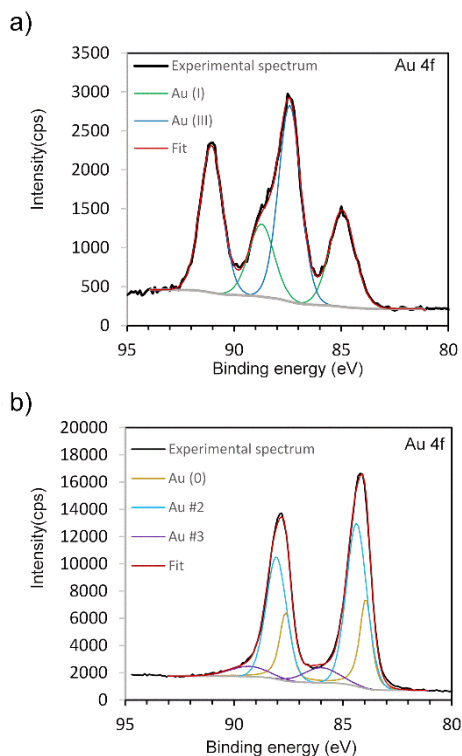


Fig.4 High resolution XPS spectra of Au 4f and Cl 2p envelopes of the deposits obtained: a) without plasma and b) with applying plasma during deposition.

Another result pointing out the role of plasma, is the Cl/Au at.% ratio (Table 1), which was found to be 2.70 and 0.15 for no-plasma and plasma-treated sample, respectively. This proves that indeed, plasma enhanced the degradation of the precursor and promoted the formation of metallic Au NPs.

Table 1. XPS elemental quantification from high resolution spectra.

Sample	Au 4f, %	C 1s, %	Cl 2p, %	O 1s, %	Si 2p, %
No plasma	2.2	39.4	5.3	24.9	28.2
With plasma	8.8	49.6	1.0	31.8	8.8

#### 4. Conclusions

We report here the strong plasma effect in providing a fine dispersion of Au NPs, embedded in a carbon-based matrix. On the contrary, the deposition without plasma is

very scarce, and undesired agglomeration is present. Therefore, fabricating different composites that include Au NPs can be foreseen with the plasma deposition method described here. Our work provides a new pathway in Au NPs synthesis since the excellent dispersion of the deposit was enabled without any capping agent.

#### 5. References

- [1] M. Das, K. H. Shim, S. S. A. An, and D. K. Yi, *Toxicol. Environ. Health Sci.*, **3**, 193 (2011)
- [2] M. Yafout, A. Ousaid, Y. Khayati, and I. S. El Otmani, *Sci. African*, **11**, e00685 (2021)
- [3] K. Saha, S. S. Agasti, C. Kim, X. Li, and V. M. Rotello, *Chem. Rev.*, **112**, 2739 (2012)
- [4] A. Ahmad et al., *RSC Adv.*, **120**, 99364 (2015)
- [5] M. H. Hussain, N. F. Abu Bakar, A. N. Mustapa, K. F. Low, N. H. Othman, and F. Adam, *Nanoscale Res. Lett.*, **15**, 140 (2020)
- [6] Y. Wang et al., *Nat. Commun.*, **11**, 11:6089 (2020)
- [7] D. Mariotti, J. Patel, V. Švrček, and P. Maguire, *Plasma Process. Polym.*, **9**, 1074 (2012)
- [8] D. Sun et al., *Langmuir*, **35**, 4577 (2019)
- [9] J. P. Sylvestre, S. Poulin, A. V. Kabashin, E. Sacher, M. Meunier, and J. H. T. Luong, *J. Phys. Chem. B*, **108**, 16864 (2004)
- [10] H. Schmidbaur, *Angew. Chemie Int. Ed. English*, **15**, 728 (1976)
- [11] A. Patnaik and C. Li, *Appl. Surf. Sci.*, **140**, 197 (1999)
- [12] F. Gao and Y. Xu, *J. Appl. Polym. Sci.*, **65**, 931 (1997)
- [13] Z. X. and Y. Y. Xiping Duan, Xuelin Tian, Jinhua Ke, Yan Yin, Jianwei Zheng, Jin Chen, Zhenming Cao, *Chem. Sci.*, **7**, 3181 (2016)
- [14] N. M. Figueiredo, N. J. M. Carvalho, and A. Cavaleiro, *Appl. Surf. Sci.*, **257**, 5793 (2011)
- [15] E. D. Park and J. S. Lee, *J. Catal.*, **186**, 1 (1999)
- [16] A. Villa et al., *Chem. Soc. Rev.*, **45**, 4953 (2016)